

Hyperpolarizability dispersion measured for (CH₃)₂O

Vincent W. Couling^{1,a)} and David P. Shelton²

¹*School of Chemistry and Physics, University of KwaZulu-Natal, Private Bag X01, Scottsville, Pietermaritzburg 3209, South Africa*

²*Department of Physics and Astronomy, University of Nevada, Las Vegas, Nevada 89154-4002, USA*

(Received 2 October 2015; accepted 18 November 2015; published online 8 December 2015)

The third-order nonlinear-optical susceptibility of dimethyl ether, (CH₃)₂O, has been measured in the gas phase over the wavelength range 488 nm < λ < 1064 nm using the technique of gas-phase electric-field-induced second-harmonic generation with periodic phase matching and with N₂ as the reference gas. Measurements span a range of temperature, which allows for separation of the temperature-independent second hyperpolarizability term from the temperature-dependent first hyperpolarizability term. The dispersion curves of the isotropically averaged first and second hyperpolarizabilities (β and γ) are deduced. © 2015 AIP Publishing LLC. [<http://dx.doi.org/10.1063/1.4936865>]

I. INTRODUCTION

Experimental and theoretical study of the nonlinear optical (NLO) properties of molecules continues to attract considerable attention, a strong motivation being the search for new materials which possess the NLO properties required in the manufacture of devices for optical harmonic generation and signal processing.^{1–5} These materials are usually in the condensed phase, and undertaking quantitatively accurate predictive calculations of their NLO properties poses significant computational challenges, requiring careful consideration of several different physical effects which would not be present for isolated molecules.^{6,7}

The calculation of the first and second hyperpolarizabilities, β and γ, of small molecules in the gas phase currently allows for the assessment of new methods in *ab initio* molecular property calculations.^{4,6,8–13} These latest methods typically utilize large basis sets together with the inclusion of electron correlation and vibrational contributions. Accurate experimental values of the molecular hyperpolarizabilities for isolated molecules can in turn serve as useful benchmarks against which to assess the effects arising from the application of higher levels of *ab initio* computational theory.

Refinement of the *ab initio* quantum computational techniques so that they adequately describe the molecular hyperpolarizabilities for isolated molecules is a crucial step towards the development of suitable techniques for the calculation of NLO properties in the condensed phase.

Experimental data for the hyperpolarizabilities of polyatomic molecules in the gas-phase are somewhat limited.^{4,14,15} The purpose of this investigation is to present electric-field-induced second-harmonic generation (ESHG or EFISH) experimental measurements of the dispersion of the isotropically averaged first and second hyperpolarizabilities of the dimethyl ether (DME) molecule (CH₃)₂O in the gas phase. DME was selected since recent state-of-the-art high-level *ab initio* computational methods have been employed to calculate spectroscopic properties of this molecule,¹⁶ so that

these methods could be profitably applied by computational chemists to calculate its NLO properties. This would allow for the insightful comparison of experiment and theory for the NLO properties of a smaller polyatomic molecule. The recent interest in calculating and measuring the spectroscopic properties of DME (see, for example, Refs. 16 and 17 and the references therein) has arisen primarily because the molecule is of astrophysical relevance, first having been detected in emission from the Orion Nebula,¹⁸ and subsequently being found to be abundant in star-forming regions.¹⁹

II. THEORY

The third-order nonlinear susceptibility $\chi^{(3)}(-2\omega; \omega, \omega, 0)$ mediates a wide range of nonlinear optical processes.^{1,20–22} A comprehensive review of the theory of gas-phase ESHG measurement has been provided⁴ and so is only briefly summarized here. Experimental measurement of ESHG yields $\chi^{(3)}(-2\omega; \omega, \omega, 0)$, which is related to the thermally averaged microscopic second hyperpolarizability Γ by

$$\chi^{(3)}(-2\omega; \omega, \omega, 0) = \frac{1}{4} \mathcal{L}_\omega \mathcal{L}_\omega^2 \mathcal{L}_{2\omega} \rho \Gamma. \quad (1)$$

Here, $\mathcal{L}_\omega = (n_\omega^2 + 2)/3$ is the Lorentz local field factor (n_ω being the refractive index) at frequency ω , while ρ is the molecular number density. For a dipolar molecule like DME in the presence of static and optical electric fields with parallel polarizations, Γ is

$$\Gamma = \gamma_{\parallel} + \frac{\mu_0 \beta_{\parallel}}{3kT}, \quad (2)$$

where γ_{\parallel} is the scalar component of the second hyperpolarizability, μ_0 is the permanent dipole moment, k is Boltzmann's constant, T is the absolute temperature, and β_{\parallel} is the component of β in the direction of the dipole moment.

Γ in Eq. (2) arises from two separate contributions, namely, the temperature-independent second-hyperpolarizability term that has its source in the distortion of the electronic structure by the applied electric field and the temperature-dependent first-hyperpolarizability term due to

^{a)}Electronic mail: couling@ukzn.ac.za

the orientational effect of the electric field on the permanent dipole moment. Consequently, for a dipolar molecule like DME, it is necessary to take ESHG measurements over a suitable range of temperature if the separation of these two terms is to be achieved.

β_{\parallel} expressed in terms of the components of the tensor β is

$$\beta_{\parallel} = \frac{1}{5} \sum_i (\beta_{zii} + \beta_{izi} + \beta_{iiz}) = \frac{3}{5} \beta_z, \quad (3)$$

while the scalar component of the second hyperpolarizability tensor is given by the isotropic average

$$\gamma_{\parallel} = \frac{1}{15} \sum_{ij} (\gamma_{iijj} + \gamma_{ijji} + \gamma_{ijij}). \quad (4)$$

For the sake of simplicity, the measured hyperpolarizabilities will simply be referred to as β and γ , where $\beta = \beta_{\parallel}$ and $\gamma = \gamma_{\parallel}$.

It is important to be aware that alternative conventions for the definitions of the molecular hyperpolarizabilities exist,²³ sometimes leading to confusion in the literature, especially where differently defined hyperpolarizabilities are to be compared.

III. EXPERIMENT

The ESHG apparatus used in this experiment is essentially similar to that which has previously been described in detail,^{14,24–28} though with a few minor modifications.

For the 488.0 nm and 514.5 nm visible incident wavelengths, a cw laser beam from an argon-ion laser is used, the beam being weakly focused through a cylindrical stainless-steel cell containing the gas sample together with the electrode array which produces a symmetry-breaking dc electric field, thus allowing second-harmonic generation to occur in the gas. The pressure of the gas is adjusted until the coherence length of the gas matches the period of the electrode array, the electrodes being arranged such that the field alternates in direction for every coherence length. The consequent achievement of periodic phase matching means a maximization of signal. The electrode spacing used is 2.69 mm, and the emergent second harmonic beam is separated from the fundamental by passage through an optical cascade of a short-wave-pass dichroic beamsplitter (CVI Laser Optics, 99.5% reflection of visible radiation, >85% transmission of UV), a Schott reflection filter (UV-R-250), and three by 2 mm Schott UG-5 filters. A photomultiplier tube is used to count signal photons.

Visible incident radiation at 590.0 nm and 611.3 nm is generated by pumping a Coherent CR-599 dye laser (using Rhodamine 6G dye) with a 532 nm cw beam arising from a Coherent Verdi YAG laser. Here, the fundamental and second-harmonic beams are separated by passage through two 2 mm Schott UG-5 filters, three 2 mm Schott UG-11 filters, and a fused-silica lens.

The infra-red incident beam at 1064 nm is provided by an acousto-optically Q-switched Nd:YAG laser producing pulses which typically have a repetition rate of 2.1 kHz, a duration of 100 ns, and an energy of 1 mJ. A visible-blocking Schott RG-850 filter is placed just after the laser focusing lens to

prevent second-harmonic light generated along the beam path from entering the ESHG cell. The electrode spacing used is 5.08 mm, and the emergent second harmonic beam is separated from the fundamental by passage through a cascade of a Newport YAG 45° harmonic beamsplitter and six Schott KG-3 filters. Interference between the ESHG signal and any coherent second harmonic background generated after the ESHG cell was eliminated by alternating the sign of the voltage applied to the electrodes.

The principal difference between these experimental arrangements and those used previously^{14,24–28} is that a double-prism spectrometer has not been used here to aid in the separation of the second-harmonic from the fundamental laser beam. Consequently, it is useful to verify that the present experimental configurations adequately separate the two beams by preferentially absorbing enough of the fundamental beam photons so that they contribute negligibly to the photomultiplier count rates. This verification was achieved by measuring the ESHG of previously characterized species, namely, argon and SF₆, using nitrogen as the reference gas. Agreement of the measured second hyperpolarizabilities of argon and SF₆ were found to be within 0.2% of the previous determinations.¹⁴

The ratio of the thermally averaged hyperpolarizabilities of the sample gas DME and the reference gas N₂ (for which absolute values of the hyperpolarizability are available^{14,29}) is given by

$$\frac{\Gamma_{\text{DME}}}{\gamma_{\text{N}_2}} = \left[\frac{S_{\text{DME}}^{(2\omega)}}{S_{\text{N}_2}^{(2\omega)}} \right]^{1/2} \left[\frac{\rho_{\text{DME}} n'_{\text{DME}} V_{\text{DME}}}{\rho_{\text{N}_2} n'_{\text{N}_2} V_{\text{N}_2}} \right]^{-1}, \quad (5)$$

where $S^{(2\omega)}$ is the peak signal, ρ is the gas density under the phase matching conditions, and V is the voltage applied to the electrodes. The factor $n' = (n_{\omega}^4 n_{2\omega}^3 n_{2\omega})^{1/6}$, with n_{ω} the refractive index at frequency ω , includes the combined effects of the Lorentz local field factors $\mathcal{L}_0 \mathcal{L}_{\omega}^2 \mathcal{L}_{2\omega}$ and the refractive-index dependence of the laser beam focusing. Sample densities are calculated from measured pressures and temperatures using the virial equation of state.³⁰ Refractive indices are calculated from tables³¹ using the measured densities.

The DME used in this experiment was obtained from Sigma-Aldrich and had a purity of better than 99.8%, while the N₂ reference gas was of high purity, 99.999%. Measurements were made in coupled triplets in order to cancel drifts, and the estimated total uncertainty of a hyperpolarizability ratio measurement is the statistical uncertainty for an average of five triplets of runs convolved with the uncertainty of the density determinations arising from the 0.15% relative accuracy of the capacitance manometer. The accuracy of the ratio is generally around $\pm 0.3\%$ – $\pm 1\%$.

Since the linear polarizability dispersion $\Delta\alpha(\omega) = \alpha(2\omega) - \alpha(\omega)$ is proportional to ρ^{-1} , the hyperpolarizability measurements also yield the ratio of the linear polarizability dispersion $\Delta\alpha_{\text{DME}}/\Delta\alpha_{\text{N}_2}$.²⁴

IV. RESULTS AND DISCUSSION

The temperature dependence of the ratios $\Gamma_{\text{DME}}/\gamma_{\text{N}_2}$ measured at each of the five wavelengths used in the ESHG

TABLE I. ESHG data for phase-match densities and hyperpolarizability ratios at the experimental wavelengths used in this study.

λ (nm)	ν (cm ⁻¹)	T (°C)	ρ_{N_2}/ρ_{DME}	$\Gamma_{DME}/\gamma_{N_2}$
1064	9395	21.3	4.701 ± 0.011	-8.985 ± 0.021
		63.0	4.698 ± 0.011	-6.837 ± 0.020
		123.0	4.706 ± 0.012	-4.450 ± 0.018
		199.2	4.686 ± 0.015	-2.273 ± 0.007
611.3	16355	22.6	4.791 ± 0.011	-9.779 ± 0.042
		65.1	4.789 ± 0.011	-7.348 ± 0.035
		123.9	4.796 ± 0.011	-4.387 ± 0.038
590.0	16944	22.2	4.831 ± 0.011	-9.981 ± 0.050
		64.2	4.827 ± 0.011	-7.365 ± 0.092
		125.2	4.810 ± 0.011	-4.417 ± 0.050
514.5	19430	23.2	5.076 ± 0.012	-10.319 ± 0.030
		63.8	5.078 ± 0.011	-7.387 ± 0.033
		125.2	5.065 ± 0.011	-4.386 ± 0.025
		198.3	5.030 ± 0.011	-1.508 ± 0.015
488.0	20487	23.0	5.222 ± 0.012	-10.516 ± 0.063
		64.2	5.225 ± 0.012	-7.473 ± 0.053
		125.4	5.219 ± 0.013	-4.053 ± 0.072
		158.5	5.210 ± 0.012	-2.615 ± 0.061

experiment is presented in Table I. As previously done,^{28,32} the cell was enclosed in an oven, permitting measurements over a range of gas temperatures up to 200 °C, except for those wavelengths where the higher temperatures yielded unacceptably low count rates for DME. Also presented in Table I are the density ratios ρ_{N_2}/ρ_{DME} , which provide the experimentally measured linear polarizability dispersion ratio values via $\rho_{N_2}/\rho_{DME} \approx \Delta\alpha_{DME}/\Delta\alpha_{N_2}$.

The hyperpolarizability ratios at a wavelength of 1064 nm are plotted in Fig. 1 to illustrate the linear variation with T^{-1} as predicted by Eq. (2). The relative first and second hyperpolarizabilities of DME with respect to N_2 are obtained

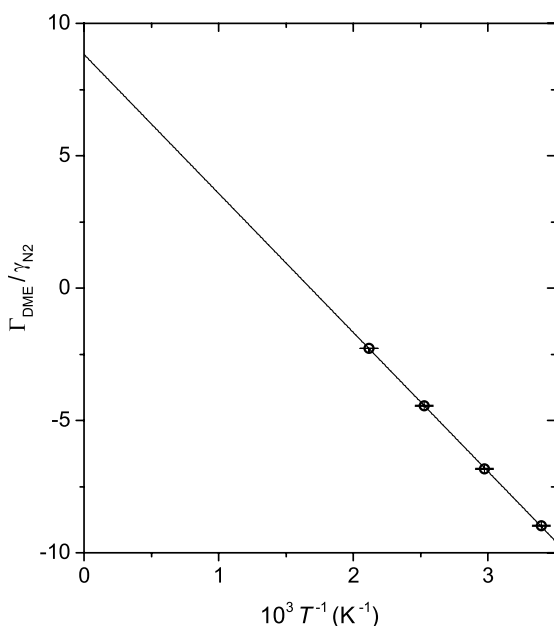


FIG. 1. A plot of the hyperpolarizability ratios $\Gamma_{DME}/\gamma_{N_2}$ vs the inverse absolute temperature for DME at a wavelength of 1064 nm.

from a weighted least-squares straight-line fit to the values of $\Gamma_{DME}/\gamma_{N_2}$ plotted vs T^{-1} . The slopes and intercepts of these fits are presented in Table II, together with their associated uncertainties.

The absolute values of the gas phase DME hyperpolarizabilities, which are also presented in Table II, have been extracted from the measured ratios using the previously determined absolute values of the N_2 second hyperpolarizability.^{14,29} Use has been made of the dipole moment for DME, $\mu_0 = 4.37 \pm 0.03 \times 10^{-30}$ C m,³³ in Eq. (2). Also presented in Table II are the results obtained by Ward and Miller for the first and second hyperpolarizabilities of DME obtained from their ESHG measurements using a ruby laser, wavelength 694.3 nm.³⁴

The frequency dependencies of the electronic contributions to β and γ for NLO processes may both be represented by even power series in ν_L^2 ,^{4,35-39} namely,

$$\beta(-\nu_\sigma; \nu_1, \nu_2) = \beta(0; 0, 0) [1 + A\nu_L^2 + B\nu_L^4 + \dots] \quad (6)$$

and

$$\gamma(-\nu_\sigma; \nu_1, \nu_2, \nu_3) = \gamma(0; 0, 0, 0) [1 + A'\nu_L^2 + B'\nu_L^4 + \dots], \quad (7)$$

where

$$\nu_L^2 = \nu_\sigma^2 + \nu_1^2 + \nu_2^2 + \nu_3^2. \quad (8)$$

For ESHG, one has $\gamma(-2\nu; \nu, \nu, 0)$, $\beta(-2\nu; \nu, \nu)$, and $\nu_L^2 = 6\nu^2$. These power series describe only the electronic contribution to β and γ , and not the vibrational and rotational contributions. Since the vibrational^{40,41} and rotational contributions are not expected to be large for DME, the dispersion curves should be adequately accurate over the present range of optical wavelengths. Dispersion curves have accordingly been fitted to our experimentally deduced hyperpolarizability data contained in Table II. The data of Ward and Miller³⁴ have not been included in the fits since they are inconsistent with the present results, being 70% less negative for β and 71% too low for γ . The reason for this substantial discrepancy is unclear, although the presence of a gas impurity in the DME sample of Ward and Miller is a possibility.

Writing $\gamma(0; 0, 0, 0)$ as γ_0 and $\beta(0; 0, 0)$ as β_0 , the coefficients of the weighted least-squares fits to the hyperpolarizability data in Table II are $\beta_0 = -0.2714 \times 10^{-50}$ C³ m³ J⁻², $A = 1.565 \times 10^{-10}$ cm², and $B = 9.759 \times 10^{-20}$ cm⁴ and $\gamma_0 = 0.4902 \times 10^{-60}$ C⁴ m⁴ J⁻³, $A' = 0.8573 \times 10^{-10}$ cm², and $B' = 16.96 \times 10^{-20}$ cm⁴. β_0 and γ_0 approximate the static electronic hyperpolarizabilities β_0^e and γ_0^e when the vibrational contributions to the measured hyperpolarizabilities are sufficiently small. The first and second hyperpolarizability data and fitted curves are shown in Figs. 2 and 3, respectively. It should be noted that weighted least-squares fits to the hyperpolarizability data yield coefficients which are quite sensitive to variations in the errors of the data.

The best-fit dispersion curves for both β and γ are found to lie just outside the error bars for the measured data at 488.0 nm, perhaps casting some doubt on the accuracy of these data points. If these data points are omitted altogether from the weighted fits, the resulting γ dispersion curve yields fitted coefficients of $\gamma_0 = 0.4754 \times 10^{-60}$ C⁴ m⁴ J⁻³, $A' = 1.614 \times 10^{-10}$ cm², and $B' = 14.74 \times 10^{-20}$ cm⁴, which

TABLE II. The slopes and intercepts of the weighted least-squares straight-line fits to the experimental data obtained from gas-phase ESHG measurements of DME shown in Table I, together with the first and second molecular hyperpolarizabilities for DME extracted via Eq. (2). Also tabulated are the previous results of Ward and Miller at 694.3 nm.³⁴

λ (nm)	ν (cm ⁻¹)	Slope (K ⁻¹)	Intercept	$10^{50}\beta$ (C ³ m ³ J ⁻²)	$10^{60}\gamma$ (C ⁴ m ⁴ J ⁻³)
1064	9395	-5274 ± 15	8.888 ± 0.035	-0.3013 ± 0.0008	0.5357 ± 0.0021
694.3 ^a	14399			-0.215 ± 0.004	0.393 ± 0.008
611.3	16355	-6275 ± 66	11.34 ± 0.19	-0.4107 ± 0.0043	0.7828 ± 0.0133
590.0	16944	-6357 ± 81	11.53 ± 0.24	-0.4226 ± 0.0054	0.8090 ± 0.0169
514.5	19430	-7017 ± 24	13.35 ± 0.06	-0.5026 ± 0.0017	1.0089 ± 0.0046
488.0	20487	-7462 ± 76	14.66 ± 0.22	-0.5537 ± 0.0061	1.1484 ± 0.0170

^aFrom ESHG measurements in Ref. 34.

appear to be more physically reasonable, considering the coefficients previously obtained for propane,¹⁴ namely, $A' = 2.132 \times 10^{-10}$ cm² and $B' = 6.667 \times 10^{-20}$ cm⁴. Propane and DME have comparable values for both γ and the polarizability dispersion (indicated by ρ_{N_2}/ρ_X), as shown in Table III. The β dispersion curve coefficients obtained after omitting the 488.0 nm data point are $\beta_0 = -0.2677 \times 10^{-50}$ C³ m³ J⁻², $A = 1.908 \times 10^{-10}$ cm² and, $B = 8.670 \times 10^{-20}$ cm⁴.

Bond additivity schemes have been proposed for β and γ .^{21,41-46} For γ , a scalar additivity scheme applies and has met with limited success.⁴³⁻⁴⁶ In Table III, the hyperpolarizabilities for several relevant molecules deduced from gas-phase ESHG measurements are compared. γ_{D_2O} and γ_{CH_3OD} yield $\gamma_{O-CH_3} = 0.181 \times 10^{-60}$ C⁴ m⁴ J⁻³, while $\gamma_{(CH_3)_2O}$ yields $\gamma_{O-CH_3} = 0.268 \times 10^{-60}$ C⁴ m⁴ J⁻³, a discrepancy of 48%. To a reasonable approximation, γ for the molecules in Table III is seen to double with each added methyl group.

The bond additivity scheme has been even less successful in predicting molecular β values,⁴³⁻⁴⁶ which

is not unexpected, since β arises from the distortion of atomic charge distributions. For β , a vector additivity scheme applies. Here, $\beta_{CH_3OD} = \frac{1}{2}\beta_{D_2O} + \frac{1}{2}\beta_{(CH_3)_2O}$. The measured $\beta_{CH_3OD} = -0.100 \times 10^{-50}$ C³ m³ J⁻² is 79% discrepant with $\frac{1}{2}\beta_{D_2O} + \frac{1}{2}\beta_{(CH_3)_2O} = -0.179 \times 10^{-50}$ C³ m³ J⁻², which is not very satisfactory.

At present, the vibrational contributions to β and γ for DME are unknown. *Ab initio* computations for CH₄ yield ESHG vibrational contributions to β and γ in the visible of around 1% and 0.6%, respectively.^{40,41} Since γ for DME is approximately that of two CH₄ molecules (see Table III), the relative vibrational contributions to γ for DME may be similar to those for CH₄, but this may not be the case for β because of the strongly polar nature of DME as compared to CH₄.

Dc Kerr-effect experiments have been performed on DME at a wavelength of 632.8 nm.^{48,49} The analysis of the data in the study of Bogaard *et al.*⁴⁸ utilized the ESHG γ of Ward and Miller³⁴ to deduce a dc Kerr β_K

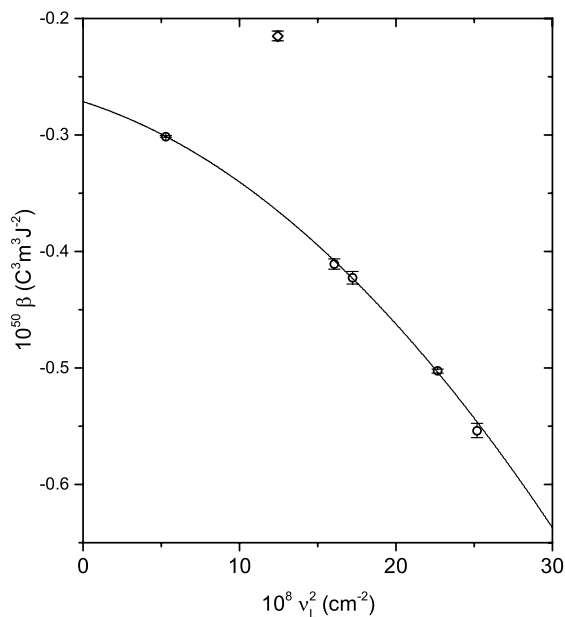


FIG. 2. The dispersion curve of the first hyperpolarizability β as a function of ν_L^2 for DME from gas-phase ESHG measurements. The solid curve is a weighted least-squares fit of the function $\beta = \beta_0[1 + A\nu_L^2 + B\nu_L^4]$ to the present data. The result of Ref. 34 at 694.3 nm is included as a diamond and lies 70% from the dispersion curve.

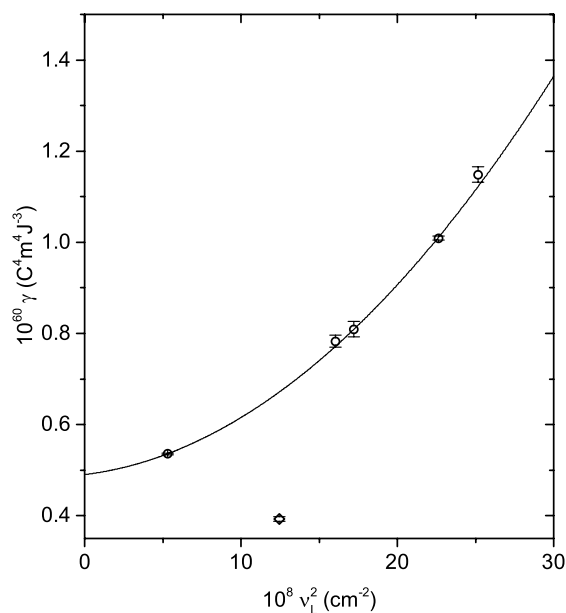


FIG. 3. The dispersion curve of the second hyperpolarizability γ as a function of ν_L^2 for DME from gas-phase ESHG measurements. The solid curve is a weighted least-squares fit of the function $\gamma = \gamma_0[1 + A'\nu_L^2 + B'\nu_L^4]$ to the present data. The result of Ref. 34 at 694.3 nm is included as a diamond and lies 71% from the dispersion curve.

TABLE III. Comparison of the results of gas-phase ESHG measurements for several molecules at the wavelength 1064 nm.

Molecule	ρ_{N_2}/ρ_X	μ_0 (D) ^a	$10^{50}\beta$ (C ³ m ³ J ⁻²)	$10^{60}\gamma$ (C ⁴ m ⁴ J ⁻³)
H ₂ O ^b	1.35	1.85	-0.062	0.112
D ₂ O ^b	1.20	1.81	-0.057	0.104
CH ₃ OD ^b	2.57	1.70	-0.100	0.233
(CH ₃) ₂ O ^c	4.70	1.30	-0.301	0.536
(CH ₃) ₂ CH ₂ ^d	5.44	0.086		0.551 ^e
CH ₄ ^d	2.17	0	0.032 ^f	0.177

^aReference 47.^bReference 28.^cThis work.^dReference 14.^eObtained assuming $\frac{\mu_0\beta}{3kT}$ to be negligible compared to γ .^f β_{xyz} , Ref. 15.

of $\beta_K = (+0.3 \pm 0.6) \times 10^{-50} \text{ C}^3 \text{ m}^3 \text{ J}^{-2}$. It is clear that β_K is inadequately determined by these Kerr-effect measurements, primarily because the contribution of β_K to the low-density molar Kerr constant is rather small. Eqs. (6) and (7) hold for the hyperpolarizabilities deduced from the dc Kerr effect, with $\gamma(\nu; \nu, 0, 0)$, $\beta(\nu; \nu, 0)$, and $\nu_L^2 = 2\nu^2$.

The more precise experimental study of Couling and Sono,⁴⁹ which was undertaken over a larger temperature range, has facilitated a more precise determination of the Kerr-effect hyperpolarizabilities. Fitting a quadratic polynomial in T^{-1} to the measured low-density molar Kerr constants yields estimates of both β_K and γ_K , namely, $\beta_K = (-0.3 \pm 0.1) \times 10^{-50} \text{ C}^3 \text{ m}^3 \text{ J}^{-2}$ and $\gamma_K = (0.12 \pm 0.3) \times 10^{-60} \text{ C}^4 \text{ m}^4 \text{ J}^{-3}$. While the determination of γ_K is inadequate, this contribution to the low-density molar Kerr constant being particularly small, the β_K , though not nearly as precise as the ESHG β , is consistent with the value at $\nu_L^2 = 4.99 \times 10^8 \text{ cm}^{-2}$ interpolated from the ESHG β dispersion curve, namely, $\beta = -0.299 \times 10^{-50} \text{ C}^3 \text{ m}^3 \text{ J}^{-2}$. (The ESHG γ dispersion curve yields a value of $\gamma = 0.532 \times 10^{-60} \text{ C}^4 \text{ m}^4 \text{ J}^{-3}$ at $\nu_L^2 = 4.99 \times 10^8 \text{ cm}^{-2}$.)

Since vibrational contributions to Kerr hyperpolarizabilities tend to be much larger than for ESHG hyperpolarizabilities,⁴ the good agreement found between the Kerr and ESHG β values for DME suggests that the vibrational contribution to β for DME is small compared to the electronic contribution at visible frequencies.

This experimental study of the ESHG of the DME molecule has provided accurate first and second hyperpolarizability dispersion curves for this polyatomic species in the gas phase. Since current high-level *ab initio* computational techniques permit the calculation of hyperpolarizabilities for smaller polyatomic molecules with inclusion of electron correlation and vibration and dispersion contributions, the availability of these new experimental benchmarks of β and γ for the DME molecule makes it a useful candidate for the assessment of state-of-the-art methods in *ab initio* molecular property calculations.

ACKNOWLEDGMENTS

V.W.C. gratefully acknowledges the award of an Ernest Oppenheimer Memorial Trust sabbatical grant.

- ¹Y. R. Shen, *Principles of Nonlinear Optics* (Wiley, New York, 1984).
- ²N. Bloembergen, *Nonlinear Optics*, 4th ed. (World Scientific, Singapore, 1996).
- ³P. N. Butcher and D. Cotter, *The Elements of Nonlinear Optics*, Cambridge Studies in Modern Optics, reprint ed. (Cambridge University Press, Cambridge, 1993).
- ⁴D. P. Shelton and J. E. Rice, *Chem. Rev.* **94**, 3 (1994).
- ⁵L. R. Dalton, *J. Phys.: Condens. Matter* **15**, R897 (2003).
- ⁶J. R. Hammond and K. Kowalski, *J. Chem. Phys.* **130**, 194108 (2009).
- ⁷A. V. Gubskaya and P. G. Kusalik, *Mol. Phys.* **99**, 1107 (2001).
- ⁸D. M. Bishop, in *Advances in Chemical Physics*, edited by I. Prigogine and S. A. Rice (Wiley, New York, 1998), Vol. 104, p. 1.
- ⁹D. M. Bishop and P. Norman, in *Handbook of Advanced Electronic and Photonic Materials and Devices, Nonlinear Optical Materials, Calculations of Dynamic Hyperpolarizabilities for Small and Medium-Sized Molecules*, edited by H. S. Nalwa (Academic Press, San Diego, 2000), Vol. 9, p. 1.
- ¹⁰*Challenges and Advances in Computational Chemistry and Physics, Nonlinear Optical Properties of Matter: From Molecules to Condensed Phases*, edited by M. G. Papadopoulos, J. Leszczynski, and A. Sadlej (Springer, New York, 2006), Vol. I.
- ¹¹T. Helgaker, S. Coriani, P. Jørgensen, K. Kristensen, J. Olsen, and K. Ruud, *Chem. Rev.* **112**, 543 (2012).
- ¹²V. Rossikhin, E. Voronkov, S. Okovytyy, T. Sergeieva, K. Kapusta, and J. Leszczynski, *Int. J. Quantum Chem.* **114**, 689 (2014).
- ¹³M. de Wergifosse, F. Castet, and B. Champagne, *J. Chem. Phys.* **142**, 194102 (2015).
- ¹⁴D. P. Shelton, *Phys. Rev. A* **42**, 2578 (1990).
- ¹⁵D. P. Shelton, *J. Chem. Phys.* **137**, 044312 (2012).
- ¹⁶M. Villa, M. L. Senet, R. Dominguez-Gomez, O. Alvarez-Bajo, and M. Carvajal, *J. Phys. Chem. A* **115**, 13573 (2011).
- ¹⁷C. P. Endres, B. J. Drouin, J. C. Pearson, H. S. P. Müller, F. Lewen, S. Schlemmer, and T. F. Giesen, *Astron. Astrophys.* **504**, 635 (2009).
- ¹⁸L. E. Snyder, D. Buhl, P. R. Schwartz, F. O. Clark, D. R. Johnson, F. J. Lovas, and P. T. Giguere, *Astrophys. J.* **191**, L79 (1974).
- ¹⁹P. Schilke, D. J. Bendford, T. R. Hunter, D. C. Lis, and T. G. Phillips, *Astrophys. J.* **132**, 281 (2001).
- ²⁰M. D. Levenson, *Introduction to Nonlinear Laser Spectroscopy* (Academic, New York, 1982).
- ²¹M. P. Bogaard and B. J. Orr, in *International Review of Science, Physical Chemistry, Molecular Structure and Properties*, edited by A. D. Buckingham (Butterworths, London, 1975), Vol. 2, p. 149.
- ²²D. C. Hanna, M. A. Yuratich, and D. Cotter, *Nonlinear Optics of Free Atoms and Molecules* (Springer, Berlin, 1979).
- ²³A. Willetts, J. E. Rice, D. M. Burland, and D. P. Shelton, *J. Chem. Phys.* **97**, 7590 (1992).
- ²⁴D. P. Shelton and A. D. Buckingham, *Phys. Rev. A* **25**, 2787 (1982).
- ²⁵V. Mizrahi and D. P. Shelton, *Phys. Rev. A* **31**, 3145 (1985).
- ²⁶D. P. Shelton, *Rev. Sci. Instrum.* **56**, 1474 (1985).
- ²⁷V. Mizrahi and D. P. Shelton, *Phys. Rev. A* **32**, 3454 (1985).
- ²⁸P. Kaatz, E. A. Donley, and D. P. Shelton, *J. Chem. Phys.* **108**, 849 (1998).
- ²⁹V. Mizrahi and D. P. Shelton, *Phys. Rev. Lett.* **55**, 696 (1985).
- ³⁰J. H. Dymond, K. N. Marsh, R. C. Wilhoit, and K. C. Wong, *The Virial Coefficients of Pure Gases and Mixtures* (Springer-Verlag, Berlin, 2002).
- ³¹*Landolt-Börnstein, Zahlenwerte und Funktionen*, edited by K.-H. Hellwege and A. Hellwege (Springer-Verlag, Berlin, 1962), Vol. II.
- ³²M. Stähelin, C. R. Moylan, D. M. Burland, A. Willetts, J. E. Rice, D. P. Shelton, and E. A. Donley, *J. Chem. Phys.* **98**, 5595 (1993).
- ³³U. Blukis, P. H. Kasai, and R. J. Myers, *J. Chem. Phys.* **38**, 2753 (1963).
- ³⁴J. F. Ward and C. K. Miller, *Phys. Rev. A* **19**, 826 (1979).
- ³⁵D. M. Bishop and D. W. de Kee, *J. Chem. Phys.* **104**, 9876 (1996).
- ³⁶D. M. Bishop and D. W. de Kee, *J. Chem. Phys.* **105**, 8247 (1996).
- ³⁷C. Hättig, *Mol. Phys.* **94**, 455 (1998).
- ³⁸C. Hättig, *Chem. Phys. Lett.* **296**, 245 (1998).
- ³⁹D. M. Bishop, *Mol. Phys.* **94**, 989 (1998).
- ⁴⁰D. M. Bishop, F. L. Gu, and S. M. Cybulski, *J. Chem. Phys.* **109**, 8407 (1998).
- ⁴¹O. Quinet and B. Champagne, *J. Chem. Phys.* **109**, 10594 (1998).
- ⁴²A. D. Buckingham and B. J. Orr, *Q. Rev., Chem. Soc.* **21**, 195 (1967).
- ⁴³A. D. Buckingham and B. J. Orr, *Trans. Faraday Soc.* **65**, 673 (1969).
- ⁴⁴R. S. Finn and J. F. Ward, *J. Chem. Phys.* **60**, 454 (1974).
- ⁴⁵J. F. Ward and I. J. Bigio, *Phys. Rev. A* **11**, 60 (1975).
- ⁴⁶C. K. Miller and J. F. Ward, *Phys. Rev. A* **16**, 1179 (1977).
- ⁴⁷*Handbook of Chemistry and Physics*, edited by W. M. Haynes 92nd ed. (CRC Press, Boca Raton, 2011).
- ⁴⁸M. P. Bogaard, A. D. Buckingham, and G. L. D. Ritchie, *J. Chem. Soc., Faraday Trans. 2* **77**, 1547 (1981).
- ⁴⁹T. J. Sono, M.Sc. thesis, University of Natal, 2003.